

Significantly enhanced structural integrity of adhesively bonded PPS and PEEK composite joints by rapidly UV-irradiating the substrates

Quan, Dong; Alderliesten, René; Dransfeld, Clemens; Tsakoniatis, Ioannis; Teixeira De Freitas, Sofia; Scarselli, Gennaro; Murphy, Neal; Ivanković, Alojz; Benedictus, Rinze

DOI

[10.1016/j.compscitech.2020.108358](https://doi.org/10.1016/j.compscitech.2020.108358)

Publication date

2020

Document Version

Final published version

Published in

Composites Science and Technology

Citation (APA)

Quan, D., Alderliesten, R., Dransfeld, C., Tsakoniatis, I., Teixeira De Freitas, S., Scarselli, G., Murphy, N., Ivanković, A., & Benedictus, R. (2020). Significantly enhanced structural integrity of adhesively bonded PPS and PEEK composite joints by rapidly UV-irradiating the substrates. *Composites Science and Technology*, 199, Article 108358. <https://doi.org/10.1016/j.compscitech.2020.108358>

Important note

To cite this publication, please use the final published version (if applicable).
Please check the document version above.

Copyright

Other than for strictly personal use, it is not permitted to download, forward or distribute the text or part of it, without the consent of the author(s) and/or copyright holder(s), unless the work is under an open content license such as Creative Commons.

Takedown policy

Please contact us and provide details if you believe this document breaches copyrights.
We will remove access to the work immediately and investigate your claim.



Significantly enhanced structural integrity of adhesively bonded PPS and PEEK composite joints by rapidly UV-irradiating the substrates

Dong Quan ^{a,*}, René Alderliesten ^a, Clemens Dransfeld ^a, Ioannis Tsakoniatis ^a, Sofia Teixeira De Freitas ^b, Gennaro Scarselli ^{b,c}, Neal Murphy ^b, Alojz Ivanković ^b, Rinze Benedictus ^a

^a Department of Aerospace Structures and Materials, Delft University of Technology, Netherlands

^b School of Mechanical and Materials Engineering, University College Dublin, Ireland

^c Department of Innovation Engineering, University of Salento, Italy

ARTICLE INFO

Keywords:

A: Adhesive joints
A: Polymer-matrix composites (PMCs)
B: Strength
B: Fracture toughness
E: Welding/joining

ABSTRACT

A high-power UV-irradiation technique was proposed for the surface treatment of PPS and PEEK composites, aiming to achieve good adhesion with epoxy adhesives. The composite substrates were rapidly UV-irradiated for a duration of between 2–30 s, and then bonded using an aerospace film adhesive to produce joints. Tensile lap-shear strength and mode-I and mode-II fracture energies of the adhesive joints were investigated. It was observed that the application of a short-time UV-irradiation to the substrates transformed the failure mode of the specimens from adhesion failure to substrate damage in all cases. This consequently resulted in remarkable improvements in the mechanical and fracture performance of the adhesive joints. For example, the lap-shear strength increased from 11.8 MPa to 31.7 MPa upon UV-irradiating the PPS composites for 3 s, and from 8.3 MPa to 37.3 MPa by applying a 5 s UV-irradiation to the PEEK composites. Moreover, the mode-I and mode-II fracture energies significantly increased from $\sim 50 \text{ J/m}^2$ to $\sim 1500 \text{ J/m}^2$ and from $<300 \text{ J/m}^2$ to $\sim 7000 \text{ J/m}^2$, respectively for both of the adhesively bonded PEEK and PPS composite joints.

1. Introduction

Carbon fibre reinforced thermoplastic composites (TPCs) offer many advantages over thermoset composites (TSCs), including a high resistance to impact and fracture damage, the ability to be re-melted and re-shaped and a low storage cost as a result of an infinite shelf life. For this reason, they are increasingly being used to replace the metallic and TSC counterparts in a wide variety of industries, including automotive, aerospace and marine sectors. Accordingly, it becomes critical to develop effective joining methods for TPCs. To date, mechanical fastening [1–3], adhesive bonding [4–7] and welding (infusion bonding) [8,9] are the major methods for joining thermoplastics and their composite materials. Additionally, Li et al. [10–12] proposed to use a variotherm injection moulding method for joining thermoplastics to Aluminium substrates. It was reported that a lap-shear strength of 25 MPa had been obtained for hybrid Polyphenylene sulphide/Aluminium joints, showing some promise for industrial application. While each of these methods has its own strengths and weakness, adhesive bonding is unique for joining thin-walled sections or elements with a significant difference in thickness [13]. Moreover, it presents many advantages over the other methods to the structural joining of FRPs, such as the

possibility of joining any pair of dissimilar materials, achieving a uniform stress-distribution along the junction between the two substrates, making light-weight constructions, and sealing the entire bonding area and hence to provide high joint strength and durability [14].

The majority of thermoplastics, including Polyether ether ketone (PEEK) and Polyphenylene sulfide (PPS), possess a low level of adhesion with epoxy adhesives due to their inherently poor reactivity, small surface energies and weak polarities [15]. Accordingly, relatively intensive surface preparation of the TPCs prior to adhesive joining is required, that could be achieved by using different methods, including acid etching [16,17], corona discharge [18,19], plasma treatment [20–22] and oxidising flame treatment [23,24]. However, there are specific limitations to each of these techniques, such as the lack of uniformity of the treated surfaces (corona discharge, plasma and oxidising flame treatments), the poor access to some small inner surfaces (corona discharge and oxidising flame treatments), the low efficiency for treating components with large surfaces (acid etching, corona discharge, plasma and oxidising flame treatments) and the acid solution is highly toxic (acid etching) etc. Ultraviolet light (UV)-irradiation was initially

* Corresponding author.

E-mail address: d.quan-1@tudelft.nl (D. Quan).

<https://doi.org/10.1016/j.compscitech.2020.108358>

Received 22 May 2020; Received in revised form 3 July 2020; Accepted 14 July 2020

Available online 18 July 2020

0266-3538/© 2020 The Authors. Published by Elsevier Ltd. This is an open access article under the CC BY license (<http://creativecommons.org/licenses/by/4.0/>).

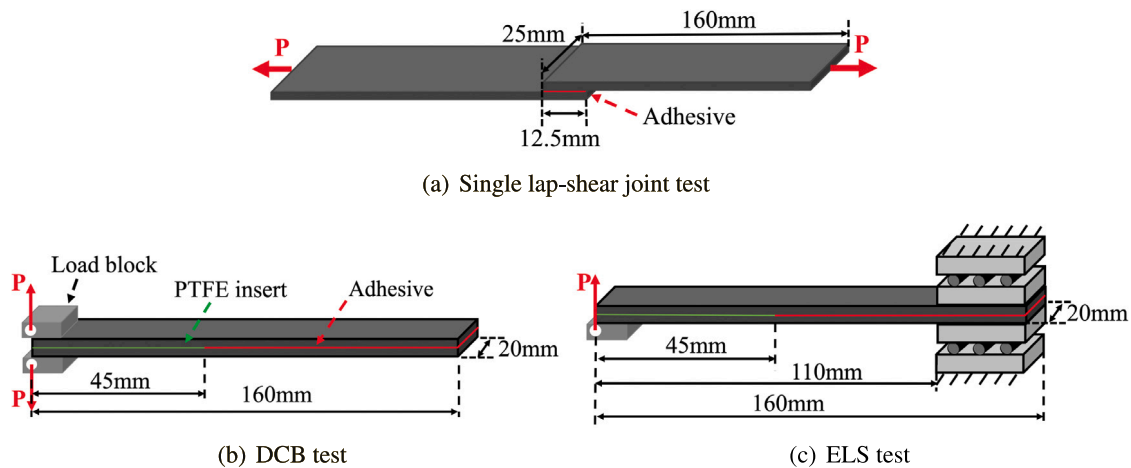


Fig. 1. Schematics of the (a) single lap-shear joint test, (b) DCB test and (c) ELS test.

developed to remove organic contaminants on the surfaces of different polymers [25]. After that, a number of studies demonstrated that applying the UV-irradiation treatment to the polymer surfaces could break the C–C bonds and also cause oxidation, chain scission and cross-linking [26,27]. Accordingly, it was often employed as an alternative surface treatment for improving the wettability of different polymer materials [28–32]. For example, Mathieson and Bradley [31] firstly used the UV-irradiation technique to activate the surfaces of PEEK and polyethylene (PE) plastics for adhesive joining. It was found that applying a UV-irradiation for a duration of between 1–10 mins significantly improved the failure loads from essentially zero to a maximum of 2 kN for the adhesive bonded PE joints, and from approximately 480 N to a maximum of 2.6 kN for the PEEK adhesive joints. The same concept was also employed by Shi et al. [32], who used UV-irradiated PEEK films as adhesives to join TSCs using a co-cure process. It was found that, upon applying a 15 min UV-irradiation to the PEEK film adhesive, the mode-I fracture behaviour of the adhesive joints transformed from a pure interfacial failure to a mix of PEEK failure and substrate damage. Consequently, the mode-I fracture energy of the adhesive joints increased from none to 820 J/m². It is worthy noting that this value was 116% higher than the interlaminar fracture toughness of the TSC substrates. The results of the literature [31,32] clearly demonstrated a high efficiency of the UV-irradiation method for the enhancement of the adhesion between thermoplastics and epoxies. However, little attention has been paid to the surface preparation of TPCs using the UV-irradiation method for the adhesive joining. Additionally, it is desirable to significantly reduce the duration of the UV-irradiation, i.e. from a few minutes [31,32] to a number of seconds to meet the requirement of mass production in industrial applications. This could be potentially achieved by using high-power UV sources, but has not been studied yet. This work investigated the effectiveness of a high-power UV-irradiation technique as a surface preparation method for the adhesive joining of carbon fibre reinforced PPS and PEEK composites. The surfaces of carbon fibre reinforced PPS and PEEK composites were rapidly UV-irradiated for a duration of between 2–30 s using a high-power UV source, and then bonded using an aerospace-grade film adhesive to produce joints. The lap shear strength and mode-I and mode-II fracture energies of the adhesive joints were studied, and the corresponding failure mechanisms were analysed.

2. Experimental

2.1. Materials and sample preparation

The carbon fibre reinforced PPS and PEEK composites were produced from 8 plies of powder-coated 5-harness satin weave prepreps,

supplied by TenCate Advanced Composites, the Netherlands. The stack sequence was $[0^\circ/90^\circ]_{4S}$, where 0° and 90° correspond to the warp and weft directions, respectively. They were consolidated in a hot-press (Joos LAP100) at 2 MPa for 30 mins. The process temperature for the PPS and PEEK composites was 320 °C and 400 °C, respectively. After the consolidation, the TPC panels were placed in a UV-irradiation chamber equipped with a LH6 MKII UV source (200 W/cm²) and a Mercury D bulb for a surface treatment lasting for between 2–30 s. In this work, the composite substrates were indicated by the type of the thermoplastic polymer followed by the duration of the UV-irradiation, e.g., PPS (None) means the non-treated PPS composites, and PPS (2sUV) indicates the PPS composite substrate that was UV-treated for 2 s. The intensities of the UV spectral ranges were determined using a UV Power Puck from EIT Inc., USA. The measured intensities of UVV (395–445 nm), UVA (320–390 nm), UVB (280–320 nm) and UVC (250–260 nm) were 1979 mW/cm², 1546 mW/cm², 343 mW/cm² and 51 mW/cm², respectively. After the UV-irradiation, two sheets of TPC laminate with one layer of film adhesive in between were assembled together and then cured in an autoclave. It should be noted that a PTFE film with a thickness of 12.5 μm was placed at desired location above the adhesive layer to introduce crack starters in the specimens for the following fracture tests. The film adhesive used for bonding the TPCs was Scotch-Weld™ AF 163-2K from 3M Netherlands B.V. This is a structural epoxy adhesive supported by a knit carrier. The curing cycle consisted of a single dwell step at 121 °C and 3 bar gauge pressure for 90 mins, and a 730 mbar under pressure inside the vacuum bag was used throughout the curing process. The average thickness of the adhesive layer within the cured adhesive joints was 136 ± 29 μm. After the curing, specimens with desired dimensions were cut out from the cured joints for the following tests.

2.2. Analysis and testing

A X-ray photoelectron spectrometer (XPS, Kratos Axis Ultra DLD) was used to determine the chemical compositions of the surfaces of the non-treated and UV-treated TPCs. The surface free energies and water contact angles of the TPC surfaces were also investigated using a mobile surface analyser from KRÜSS, GmbH. A single lap-shear joint test according to ISO4587, as schematically shown in Fig. 1(a) was used to determine the tensile lap-shear strength (LSS) of the adhesive joints. The test was carried out at a loading rate of 2 mm/min at ambient temperature. The specimens were attached to the testing machine using a pair of hydraulic clamps with a clamping pressure of 200 bar. To ensure the force was applied in the mid-plane of the adhesive layer during the lap-shear test, a misalignment between the upper and lower clamps was set. Three replicate tests were conducted for each set.

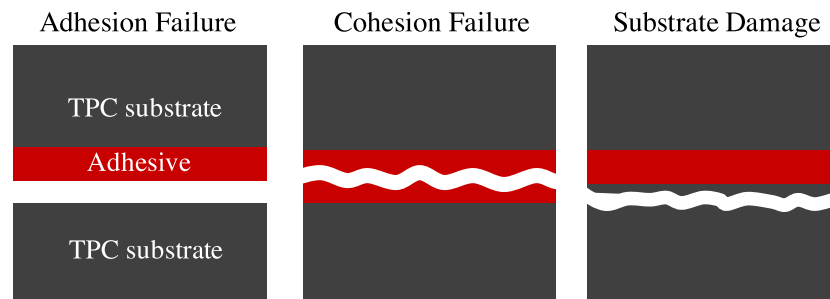


Fig. 2. Typical failure patterns of the adhesive joints.

Table 1

Results of the surface characterisations of the TPC surfaces, including carbon and oxygen content, O/C ratio, surface free energy (γ) and its polar component (γ^p), dispersive component (γ^d) and γ^p/γ^d ratio, and water contact angles (θ).

	UV-irradiation	0 s	2 s	3 s	4 s	5 s	10 s	20 s	30 s
PPS	O (%)	11.51	12.29	13.11	13.84	14.52	16.38	17.33	18.25
	C (%)	76.35	73.96	72.03	71.05	70.06	67.60	66.98	66.01
	O/C (%/%)	0.15	0.17	0.18	0.19	0.21	0.24	0.26	0.28
	γ^d (mN/m)	46.84	45.39	45.99	45.09	45.66	44.54	42.48	43.36
	γ^p (mN/m)	1.26	2.56	3.09	3.68	4.00	4.94	5.78	6.19
	γ (mN/m)	48.10	47.95	49.08	48.77	49.66	49.48	48.26	49.55
	γ^p/γ^d	0.03	0.06	0.07	0.08	0.09	0.11	0.14	0.14
	θ (°)	85.21	78.49	76.23	72.47	72.44	68.13	66.67	66.40
	PEEK	O (%)	14.93	15.68	16.49	18.05	20.04	22.97	24.04
C (%)		82.67	80.18	79.23	77.91	76.75	73.89	70.39	69.49
O/C (%/%)		0.18	0.20	0.21	0.23	0.26	0.31	0.34	0.36
γ^d (mN/m)		46.92	48.11	46.48	47.25	47.81	46.95	45.14	46.76
γ^p (mN/m)		3.64	4.76	4.98	5.13	5.87	6.14	6.31	6.50
γ (mN/m)		50.56	52.87	51.46	52.38	53.68	53.09	51.45	53.26
γ^p/γ^d		0.08	0.10	0.11	0.11	0.12	0.13	0.14	0.14
θ (°)		80.22	78.77	75.09	73.22	69.84	67.49	68.37	67.68

Table 2

Thermodynamic work of adhesion of the UV-irradiated TPC surfaces.

	UV-irradiation	0 s	2 s	3 s	4 s	5 s	10 s	20 s	30 s
PPS	W^p (mN/m)	5.72	8.16	8.96	9.78	10.19	11.33	12.26	12.69
	W^d (mN/m)	86.57	85.22	85.78	84.94	85.47	84.42	82.44	83.29
	W (mN/m)	92.29	93.38	94.74	94.72	95.66	95.75	94.70	95.97
PEEK	W^p (mN/m)	9.73	11.12	11.38	11.55	12.35	12.63	12.81	13.00
	W^d (mN/m)	86.65	87.74	86.24	86.95	87.46	86.67	84.98	86.50
	W (mN/m)	96.38	98.86	97.62	98.50	99.81	99.31	97.79	99.50

Table 3

LSSs and joint stiffnesses of the PPS and PEEK composite joints with the substrates UV-irradiated for different times.

	UV-irradiation	0 s	2 s	3 s	4 s	5 s	10 s	20 s	30 s
PPS	LSS (MPa)	11.8 ±0.3	22.4 ±0.6	31.7 ±1.5	31.2 ±0.3	30.7 ±1.3	31.4 ±1.8	32.3 ±2.2	28.9 ±0.2
	Joint stiffness (MPa)	532 ±12	555 ±16	562 ±5	562 ±3	547 ±2	550 ±8	551 ±6	566 ±15
	PEEK	LSS (MPa)	8.3 ±0.7	22.9 ±0.7	26.9 ±0.8	34.1 ±0.7	37.3 ±0.6	39.0 ±1.8	37.1 ±0.6
	Joint stiffness (MPa)	550 ±19	570 ±3	563 ±9	566 ±6	569 ±23	573 ±15	570 ±6	566 ±5

The mode-I and mode-II fracture energies of the adhesive joints were studied using a double cantilever beam (DCB) test and an end loaded split (ELS) test according to ISO15024 and ISO15114, respectively. The configurations of the DCB and ELS tests are schematically shown in Figs. 1(b) and (c). A constant displacement rate of 2 mm/min and 1 mm/min was used for the DCB tests and the ELS tests, respectively. During the fracture tests, a high resolution digital camera was used to monitor the length of the crack, that was synchronised with the load and displacement measurements based on the start time of the test. A 5 mm long precrack from the crack starter was generated by

loading the samples under an opening mode for both of the DCB and the ELS specimens. Three replicate tests were conducted in each case. The failure surfaces of the tested specimens were imaged using a VK-X1000 microscope from KEYENCE Corporation to investigate the failure mechanisms of the adhesive joints. Fig. 2 illustrates three typical failure patterns of the adhesive joints those were identified in the current work [33,34], i.e. adhesion failure (the failure took place at the TPC/epoxy interface), cohesion failure (the failure occurred within the adhesive layer) and substrate damage (the failure progressed inside the TPC substrates).

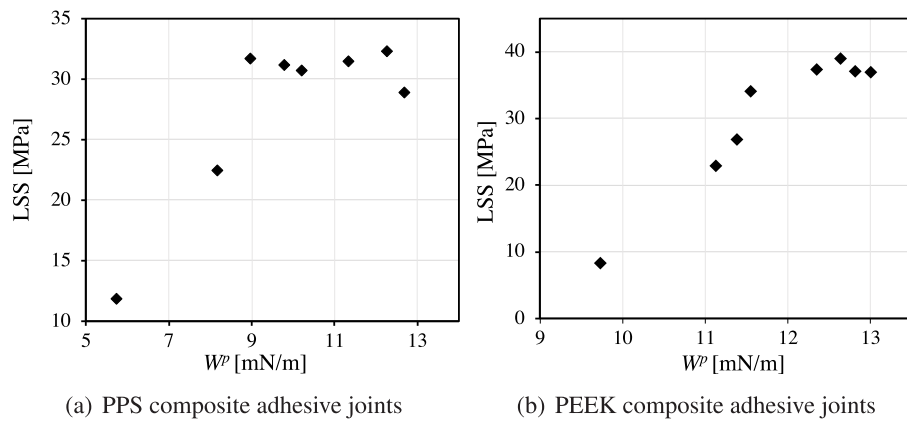
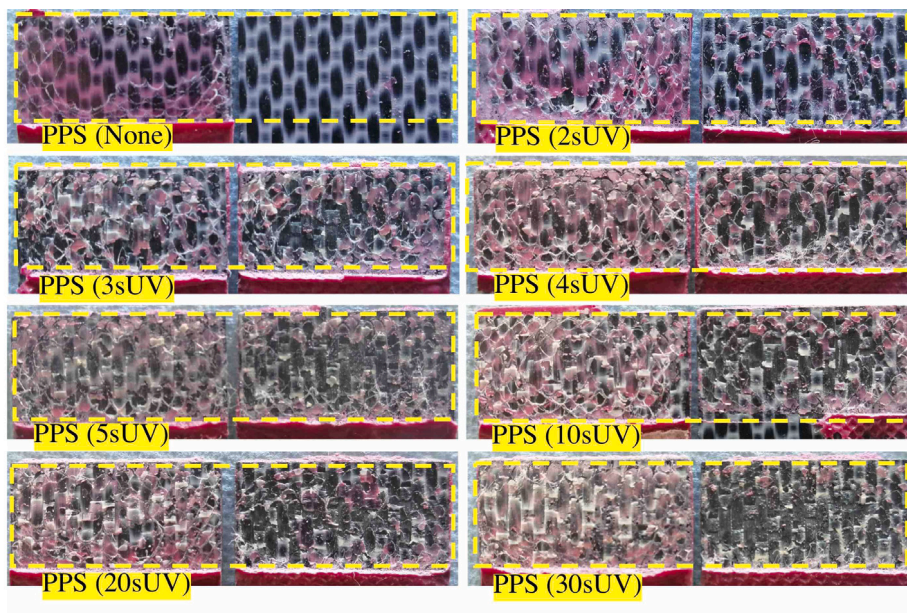
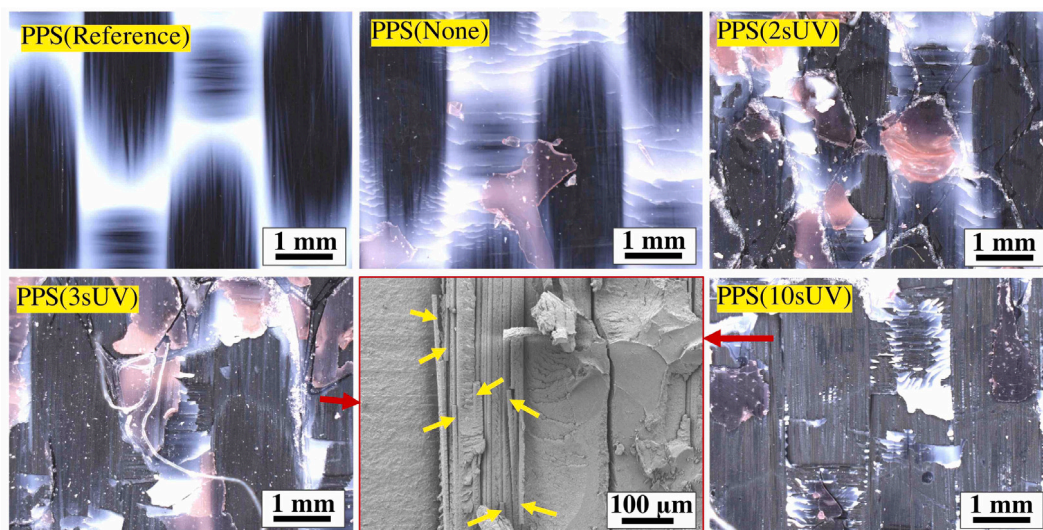


Fig. 3. LSS (lap-shear strength) versus W^p of the adhesive joints.

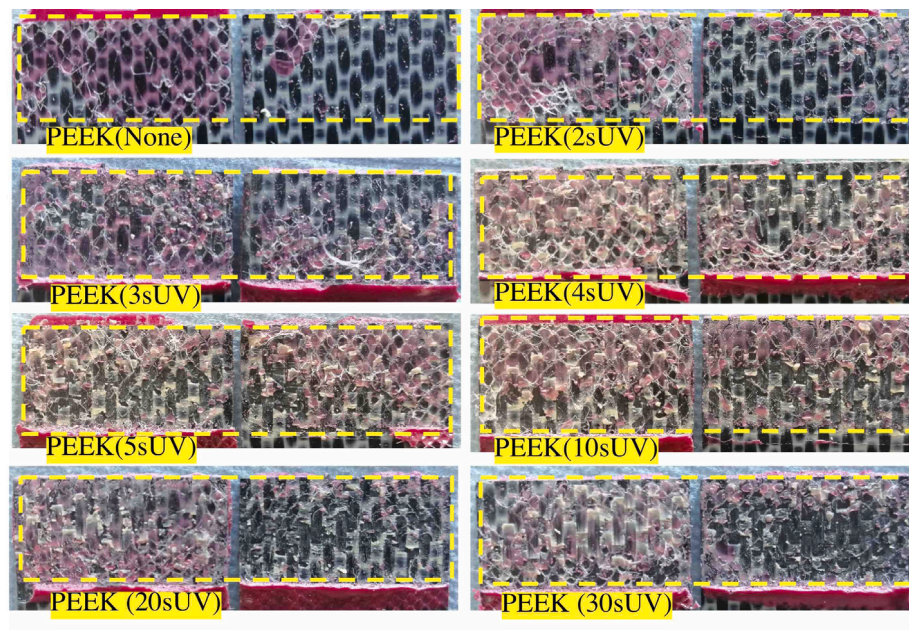


(a) Photographs

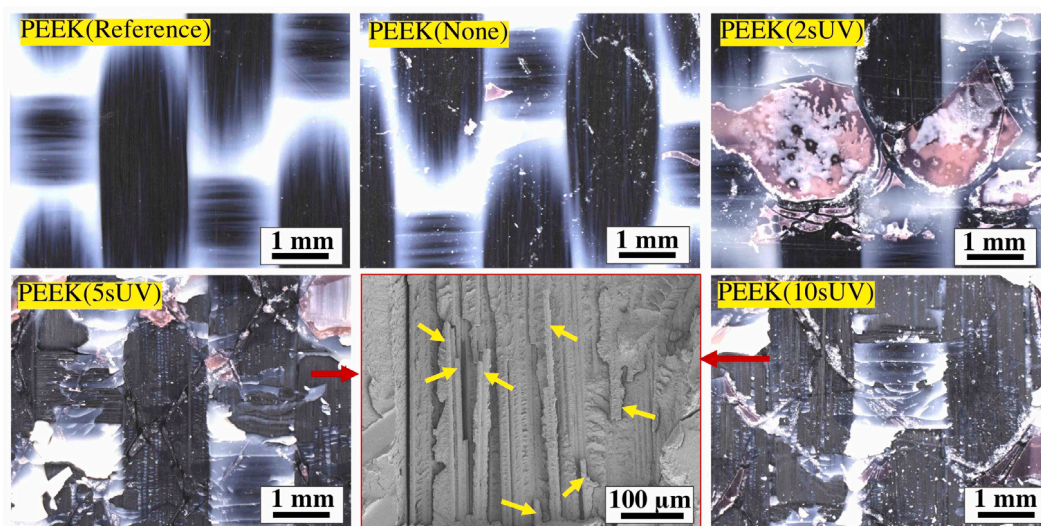


(b) Microscopy images

Fig. 4. Representative photographs and microscopy images of the failure surfaces of the lap-shear specimens of the PPS composite joints. The inset within the red box in (b) was a representative SEM image for showing the damage of the carbon fibres. The yellow arrows indicate broken carbon fibres. (For interpretation of the references to colour in this figure legend, the reader is referred to the web version of this article.)



(a) Photographs



(b) Microscopy images

Fig. 5. Representative photographs and microscopy images of the failure surfaces of the lap-shear specimens of the PEEK composite joints. The inset within the red box in (b) was a representative SEM image for showing the damage of the carbon fibres. The yellow arrows indicate broken carbon fibres. (For interpretation of the references to colour in this figure legend, the reader is referred to the web version of this article.)

3. Results and discussion

3.1. Surface characterisation

Results of the surface characterisations of the TPC surfaces are summarised in Table 1. It was found that applying a short time UV-irradiation to the TPC surfaces notably increased their oxygen contents and decreased their carbon contents for both of the PPS and PEEK composites. Consequently, the O/C ratio gradually increased from 0.15 to 0.28 for the PPS composites, and from 0.18 to 0.36 for the PEEK composites as the duration of the UV-irradiation increased up to 30 s. This was because of the high-power UV-irradiation provided sufficient energy to break the C–C/C–H species, which were associated with the development of C–O, C=O and O–C=O species to their molecular chains [31,35]. The increased amount of oxygen functional groups on the TPC surfaces subsequently affected their surface free energies. As

shown in Table 1, the application of the UV-irradiation to the TPC surfaces had no obvious effects on the dispersive component (γ^d) of the surface energy, but notably increased the polar component (γ^p) of the surface energy, i.e. γ^p increased from 1.26 mN/m to 6.19 mN/m (by 391%) for the PPS composite, and from 3.64 mN/m to 6.50 mN/m (by 79%) for the PEEK composite upon 30 s UV-irradiation. It should be noted that interactions at the interface of two phases only occur between the same type of forces, i.e. dispersive–dispersive, or polar–polar. Accordingly, a closer match between the γ^d/γ^p ratios of the TPCs and the epoxy adhesive was favoured to achieve higher level of interactions at their interface. γ^p and γ^d of epoxy adhesives were given by Kinloch [36] to be about 5–8 mN/m and 40 mN/m, respectively, corresponding to a γ^d/γ^p ratio of between 0.125–0.2. Clearly, applying the UV-irradiation to the TPCs resulted in a better match of the γ^p/γ^d ratios between the TPCs and the epoxy adhesive, see Table 1. Thermodynamic work of adhesion (W) is defined as the reversible work that is needed

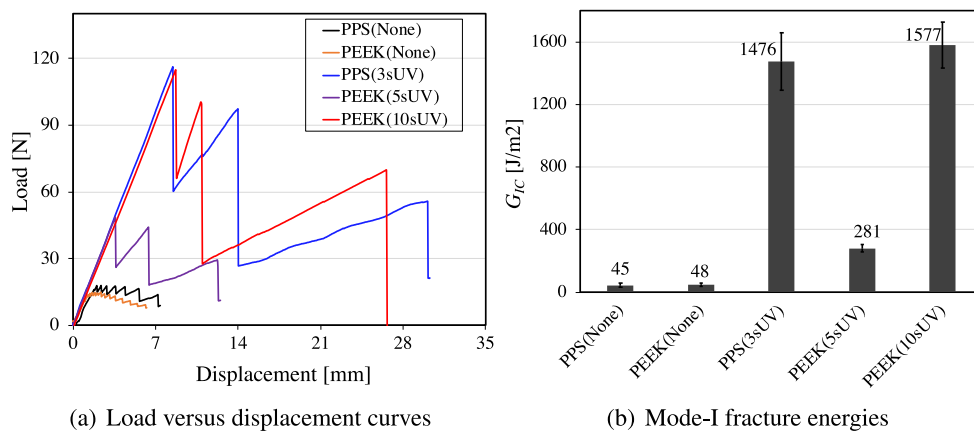


Fig. 6. Representative load versus displacement curves and corresponding mode-I fracture energies from the DCB tests of the adhesive joints.

to separate the interface from the equilibrium state of a liquid–liquid or liquid–solid phase boundary to a separation distance of infinity [37]. W between the non-cured adhesive and the TPCs can be calculated as:

$$W = W^p + W^d = 2(\gamma_a^p \gamma_s^p)^{1/2} + 2(\gamma_a^d \gamma_s^d)^{1/2} \quad (1)$$

where W^p and W^d are the contributions of the polar interactions and the dispersive interactions, respectively. The subscripts a and s denote the non-cured adhesive and the TPC substrates. The results of the calculations are presented in Table 2. Clearly, the values of W^p at the adhesive/TPC interfaces significantly increased upon UV-irradiating the TPC surfaces, while W^d exhibiting no obvious changes. It is noteworthy that, at the cured adhesive/TPC interfaces, the dispersive force was responsible for the temporary fluctuations of the charge distribution in the atoms/molecules, such as the van der Waals interactions, and the polar force generated Coulomb interactions between permanent dipoles and between permanent and induced dipoles, and subsequently generated hydrogen bonds and covalent bonds. Since hydrogen bonds and covalent bonds are much stronger than van der Waals forces, the increased values of W^p resulted in significantly improved adhesive/TPC adhesion, as will be shown in Section 3.2. As expected, the increased γ^p of the TPC surfaces significantly improved their wettability. As shown in Table 1, the water contact angles of the TPCs gradually decreased from 85.21° to 66.40° for the PPS composites and from 80.22° to 67.68° for the PEEK composites by UV-irradiating the TPCs for 30 s.

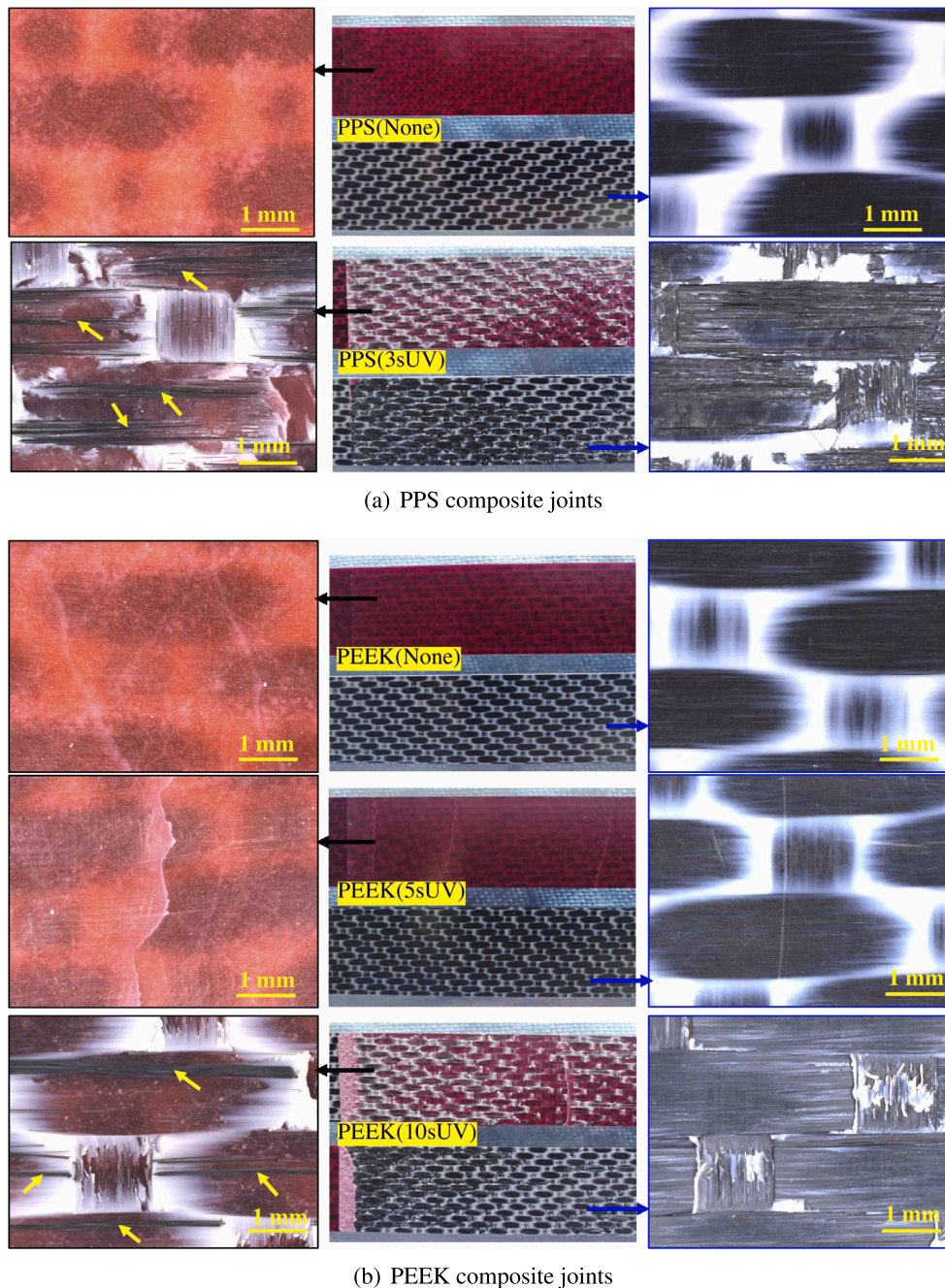
3.2. The lap-shear strength

Table 3 presents the LSSs and joint stiffnesses of the PPS and PEEK composite joints from the single lap-shear joint tests. It was found that the application of a short-time UV-irradiation to the PPS and PEEK composite substrates significantly increased the LSS of the adhesive joints, while the joint stiffness remaining unchanged. For the adhesive bonded PPS composite joints, the LSS increased from 11.8 MPa of the non-treated joints to 22.4 MPa by UV-irradiating the substrates for 2 s, and then to a plateau value of approximately 32 MPa upon a UV-irradiation of 3 s and above. A noticeable decrease in the LSS was observed as the treatment time increased from 20 s to 30 s, that was very likely due to the degradation of the mechanical properties of the PPS polymers due to an exposure to the UV-lights for a relatively long time. Similarly, the LSS of the PEEK composite joints gradually increased from 8.3 MPa of the non-treated joints to 37.3 MPa as the duration of the UV-irradiation increased to 5 s, and then remained more or less the same for a longer UV-irradiation up to 30 s. The plots of LSS versus W^p of the adhesive joints are shown in Fig. 3. It was observed that, prior to adhesive curing, W^p of about 9 mN/m and above 12 mN/m at the PPS/adhesive and PEEK/adhesive interfaces, respectively was required to achieve the plateaued LSSs of the corresponding adhesive joints.

Fig. 4(a) shows photographs of the failure surfaces of the lap-shear specimens for the PPS composite joints. An adhesion failure between the adhesive layer and the substrate was observed for the non-treated PPS composite joints, leaving a clear surface on one side of the substrates and almost the entire adhesive layer on the opposite side. The failure behaviour of the PPS composite joints transformed from an adhesion mode to a combination of adhesion and cohesion failure by applying a 2 s UV-irradiation to the substrates. As the duration of the UV-irradiation increased to 3 s and above, obvious damage to the PPS composites took place, evidenced by the presence of damaged PPS polymers on one side of the substrates and bare carbon fibres on the opposite side. Fig. 4(b) presents representative microscopy images of the failure surfaces of the PPS composite joints. A microscopy image of the PPS composite prior to adhesive bonding, i.e. PPS (Reference), is also included as a reference. The inset image with red colour outlines is a representative SEM image of the failure surfaces, focusing on the locations showing bare carbon fibres. A large number of crack lines existed inside the PPS layer on the surface of the PPS(None) substrate, indicating minor damage to the PPS polymer during the failure of the lap-shear joints. Damage to the PPS substrates became more severe upon the UV-irradiation, and as the duration of the UV-irradiation increased to 3 s and above, delaminated and broken carbon fibres occurred on the failure surfaces, as shown in the inset image of Fig. 4(b). This was attributed to the significantly improved epoxy/PPS adhesion, and explained why the LSS of the PPS composite joints became plateaued as the duration of the UV-irradiation increased to 3 s, as shown in Table 3. Photographs and microscopy images of the failure surfaces of the lap-shear specimens for the PEEK composite joints are presented in Fig. 5. Similarly to the PPS composite joints, applying the UV-irradiation to the substrates significantly affected the failure behaviour of the PEEK composite joints, i.e. the failure mode changed from an adhesion failure of the non-treated joints to a combination of adhesion and cohesion failure by applying a UV-irradiation of between 2–3 s, and further to obvious substrate damage as the duration of the UV-irradiation increased to 4 s and above, as shown in Fig. 5(a). Moreover, the damage to the PEEK substrates became more prominent as the duration of the UV-irradiation increased, and obvious carbon fibre delamination and breakage took place as the treatment time increased to 5 s and above, see Fig. 5(b). Overall, it is clear that applying a rapid UV-irradiation, i.e. 3 s for the PPS composites and 5 s for the PEEK composites, significantly improved the adhesion between the epoxy matrix and the TPC substrates to a level that was sufficiently high to cause significant damage to the TPC substrates during the lap-shear tests.

3.3. Fracture behaviour of the adhesive joints

As observed in Section 3.2, the LSS of the adhesive joints plateaued at a treatment time of 3 s for the PPS composites and 5 s for the PEEK



(a) PPS composite joints

(b) PEEK composite joints

Fig. 7. Fracture surfaces of the DCB specimens of the adhesive joints. The yellow arrows indicate some bundles of delaminated and broken carbon fibres. (For interpretation of the references to colour in this figure legend, the reader is referred to the web version of this article.)

composites. Herein, fracture test specimens underwent the same duration of UV-irradiation were also prepared and tested to evaluate the fracture response of the corresponding adhesive joints. However, the mode-I fracture energy of the adhesive bonded PEEK(5sUV) substrates was determined to be relatively low, as shown in the following section. Hence, an additional set of specimens those were UV-irradiated for 10 s, i.e. PEEK(10sUV) joints were manufactured and tested for the DCB tests.

3.3.1. Mode-I fracture behaviour

Representative load versus displacement curves from the DCB tests are shown in Fig. 6(a). It was found that the fracture loads of the DCB specimens for the non-treated TPC joints were very low, i.e. below 20 N in all cases. This was typical for the adhesively bonded PEEK and PPS

joints, owing to the inherent low surface activities of the thermoplastic matrix [32,38–40]. The crack propagated in a stick-slip manner for all the UV-treated adhesive joints, indicated by the zigzag shape of the load-versus displacement curves in Fig. 6(a). In this case, only the peak loads on the load-versus displacement curves were used to calculate the mode-I fracture energies, G_{IC} . Clearly, the application of a UV-irradiation to the TPCs significantly increased the fracture propagation load of the adhesive joints, that corresponded to remarkable increases in G_{IC} , as shown in Fig. 6(b). One can see that the application of a 3 s UV-irradiation to the PPS composite substrates remarkably increased G_{IC} from 45 J/m² of the PPS(None) joints to 1476 J/m² of the PPS(3sUV) joints. However, G_{IC} of the PEEK(5sUV) joints was measured to be 281 J/m², that was relatively low when compared to the PPS(3sUV) joints. Fortunately, this value significantly increased to

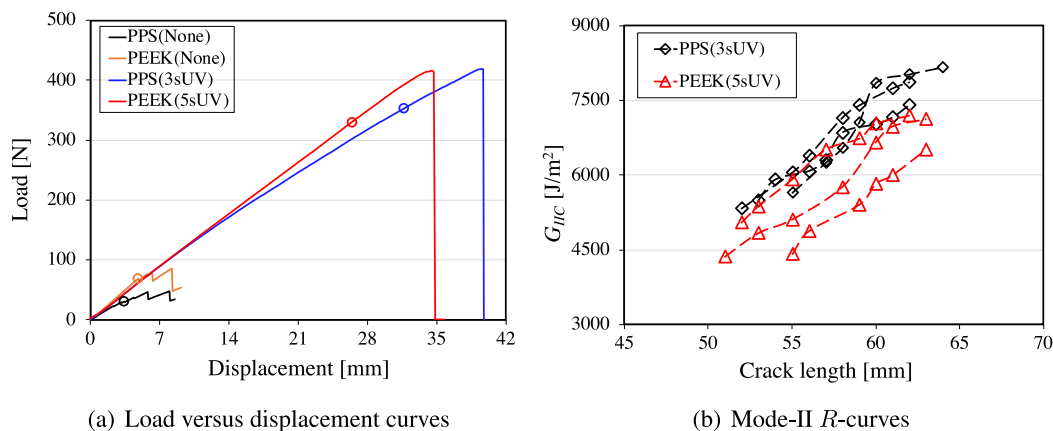


Fig. 8. Representative load versus displacement curves and mode-II R -curves from the ELS tests of the adhesive joints. The points in (a) are where crack initiation took place.

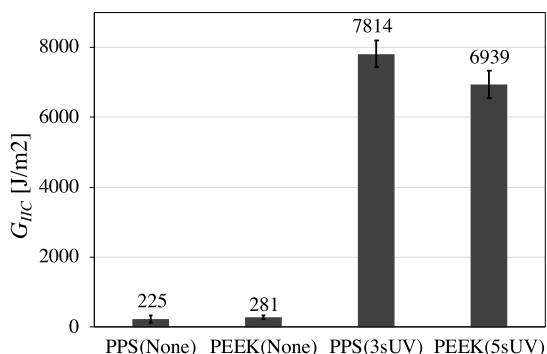


Fig. 9. Mode-II fracture energies of the adhesive joints.

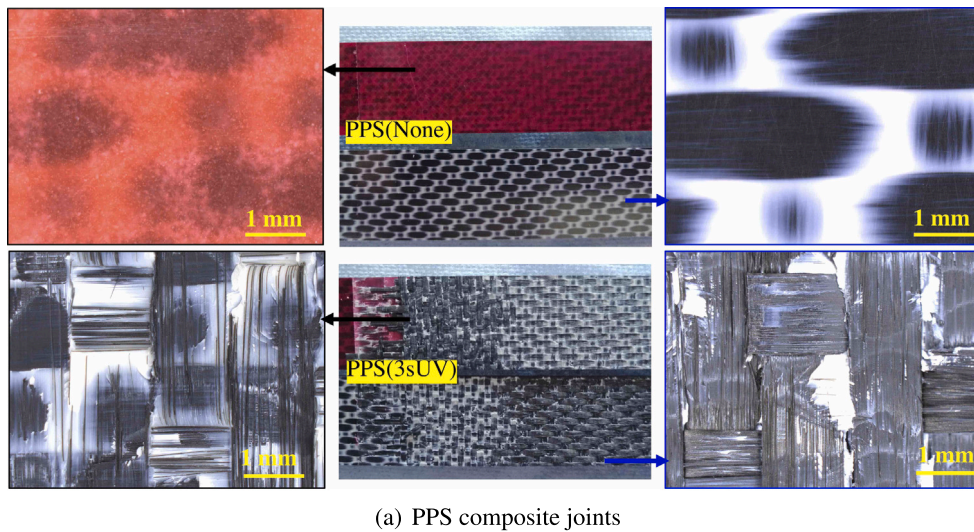
1577 J/m² as the duration of the UV-irradiation increased to 10 s. The fracture surfaces of the DCB specimens were analysed to investigate the fracture mechanisms of the adhesive joints, as shown in Fig. 7. As expected, both of the PPS(None) and PEEK(None) joints exhibited a pure adhesion failure without causing any damage to the adhesives and the TPC substrates. A number of white colour marks appeared on the adhesive layer of the PEEK(5sUV) joint, leaving corresponding white colour lines on the opposite side. These features corresponded to the peaks on the corresponding load-versus displacement curves in Fig. 6(a), and indicate some interactions between the epoxy adhesive and the PEEK(5sUV) substrate induced by the UV-irradiation. However, no other noticeable damage was observed, and this resulted in the relatively little improvements in G_{IC} of the PEEK(5sUV) joints, as shown in Fig. 6(b). For the PPS(3sUV) and PEEK(10sUV) joints, the entire adhesive layer attached on one side of the fracture surfaces, on which, extensive thermoplastic polymers and numerous broken carbon fibres were observed. Consequently, only a small amount of thermoplastic polymers remained on the surfaces of the opposite-side substrates, and the majority of the surfaces were featured with bare and damaged carbon fibres, see Fig. 7. This means the crack propagation took place in the TPC substrates, i.e. mainly at the interface between the TPC polymers and the carbon fibres. These phenomena contributed to the energy dissipation during the fracture process, and led to significant improvements in the mode-I fracture performance of the adhesive joints.

3.3.2. Mode-II fracture behaviour

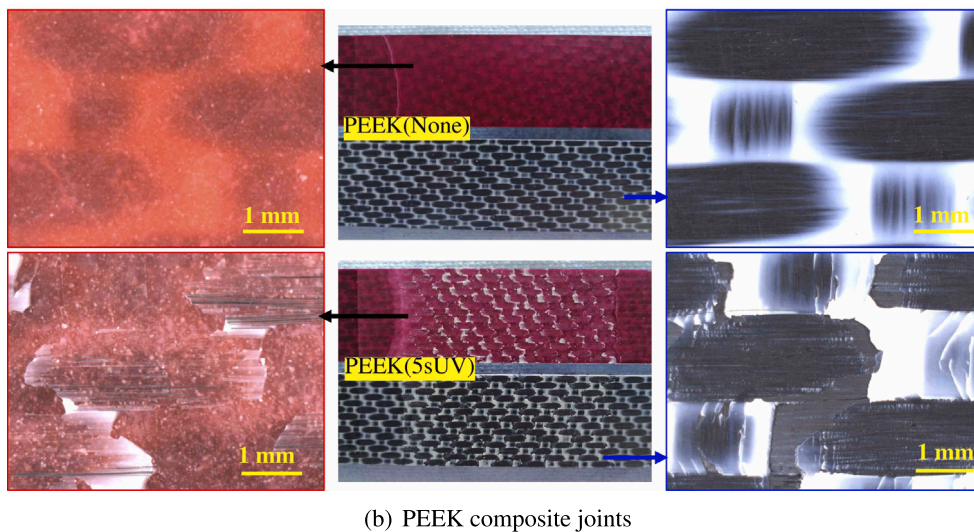
Fig. 8 shows representative load versus displacement curves and R -curves from the ELS tests of the adhesive joints. The R -curves for the non-treated joints were not shown, as the values of the fracture energy were very low. It was found that the maximum fracture propagation

load increased from below 100 N to above 400 N in both cases upon applying a rapid UV-irradiation to the PPS and PEEK composite substrates, see Fig. 8(a). It should be noted that the crack propagated for a length of approximately 10 mm and then dynamically failed the entire ELS specimens during the fracture test for all the UV-treated adhesive joints. For this reason, only the fracture energies corresponding to a crack length of between 50–65 mm were obtained on the mode-II R -curves of the adhesive joints in Fig. 8(b). It was observed that the mode-II R -curves of all the UV-treated adhesive joints exhibited a ‘rising’ behaviour, indicating an extension in the length of the mode-II fracture damage zone before the dynamic failure. Herein, the fracture energies corresponding to the last points of the R -curves, corresponding to the mode-II fracture energies at the instant of the dynamic failure of the ELS specimens, were taken as the mode-II fracture energies, G_{IIc} of the adhesive joints, which are summarised in Fig. 9. It was found that G_{IIc} increased from below 300 J/m² of the non-treated adhesive joints to 7814 J/m² of the PPS(3sUV) joints and 6939 J/m² of the PEEK(5sUV) joints. The significantly improved mode-II fracture performance could be correlated to the fracture mechanisms of the adhesive joints. Fig. 10 presents photographs and microscopy images of the fracture surfaces of the ELS specimens. It was observed that the mode-II fracture mode of the adhesive joints transformed from pure adhesion failure of the non-treated joints to significant substrate damage upon applying the UV-irradiation to the TPC substrates in both cases. Inter-ply delamination, i.e. the crack propagation path diverted from the mid-plane to the adjacent interlaminar during the fracture process, took place for the PPS(3sUV) joints, causing severe damage to both sides of the substrates, as shown in Fig. 10. For the PEEK(5sUV) joints, the entire adhesive layer together with a large number of damaged PEEK polymers and carbon fibres were observed on one side of the substrates, leaving obviously damaged PEEK layer and bare carbon fibres on the opposite side. Obviously, more severe damage to the substrates took place for the PPS(3sUV) joints than the PEEK(5sUV) joints, that resulted in a higher G_{IIc} of the PPS(3sUV) joints, as shown in Fig. 9.

Interestingly, the application of 5 s UV-irradiation to the PEEK composites only slightly improved the mode-I fracture behaviour of the adhesive joints (see Fig. 6), showing a clear adhesion failure of the PEEK(5sUV) joints, as shown in Fig. 7(b)). However, under mode-II fracture, the adhesion at the PEEK/adhesive interface of the PEEK(5sUV) joint was sufficiently high to cause damage to the substrate, and consequently resulted in remarkable improvements in the mode-II fracture behaviour. This was attributed to the different loading mode applied to the bonds at the PEEK/adhesive interface, as schematically shown in Fig. 11. During the mode-II fracture process, the bonds began to break one by one as the applied force F approached the tensile strength of the bonds. Prior to the mode-II crack propagation, the unbroken bonds were still holding the two surfaces together (as shown

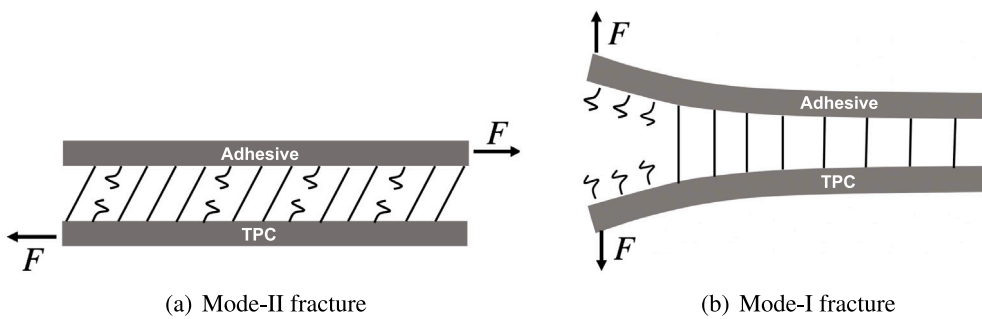


(a) PPS composite joints



(b) PEEK composite joints

Fig. 10. Fracture surfaces of the ELS specimens of the adhesive joints.



(a) Mode-II fracture

(b) Mode-I fracture

Fig. 11. Schematics for illustrating the state of the bonds under shearing (mode-II fracture) and opening (mode-I fracture) load.

in Fig. 11(a)) and the intimate contact of the two surfaces allowed some of the broken bonds recombined to create new bonds [41]. This subsequently enhanced the overall mode-II fracture performance of the adhesive joints. However, bond recombination was unexpected during the mode-I fracture process due to its opening characteristic, as schematically shown in Fig. 11(b). The opening characteristic of the mode-I fracture also negatively affected the activation energy required to break the bonds. Fig. 12 shows the Morse potentials for the unstretched and stretched bonds [41]. It was found that stretching the bond could considerably reduce the required energy to break it.

The bonds were stretched to a higher level under an opening load than a shearing load prior to the crack passing them. Accordingly, the bonds exhibited a better resistance to the mode-II fracture propagation than the mode-I fracture propagation. Moreover, it is well-known that the length of the fracture damage zone ahead of the crack tip is much longer for the mode-II fracture than the mode-I fracture [42,43], e.g., Fan et al. [43] numerically investigated the lengths of the mode-I and mode-II damage zone of a composite adhesive joint to be 0.77 mm and 9.5 mm, respectively. A significantly longer mode-II damage zone included more active bonds during the fracture process of the mode-II

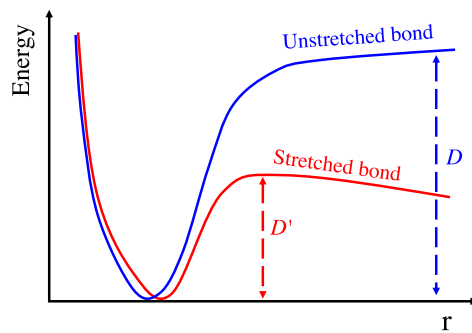


Fig. 12. Morse potentials for unstretched and stretched bonds. D and D' were the original activation energy required to break the corresponding bond [41].

fracture than the mode-I fracture. This amplified the positive influences of the bond recombination and the lower bond-stretching to the mode-II fracture energies, and subsequently resulted in the much better mode-II fracture performance than the mode-I fracture performance of the PEEK(5sUV) joints

4. Conclusions

This work proposed to use a high-power UV-irradiation technique to rapidly prepare the surfaces of carbon fibre reinforced PPS and PEEK composites for the adhesive joining. The results of a single lap-shear joint test demonstrated that applying UV-irradiation to the PPS composites for 3 s and to the PEEK composites for 5 s was sufficient to transform the failure mode of the adhesive joints from interface failure to severe substrate damage. This consequently resulted in significant increases in the lap-shear strength of the adhesive joints, i.e. from 11.8 MPa to 31.7 MPa of the PPS composite joints, and from 8.3 MPa to 37.3 MPa of the PEEK composite joints. The application of the UV-irradiation to the substrates also led to significant substrate damage during the mode-I and II fracture process of the adhesive joints, owing to the significantly enhanced adhesion at the adhesive/substrate interface. This remarkably improved the mode-I and mode-II fracture performance of the adhesive joints. For example, applying a 3 s UV-irradiation to the PPS composites significantly increased the mode-I fracture energy of the adhesive joints from 45 J/m^2 to 1476 J/m^2 , and the mode-II fracture energy from 225 J/m^2 to 7814 J/m^2 . Overall, this work demonstrated that a high structure integrity of adhesively bonded PPS and PEEK composite joints could be created by rapidly UV-irradiating the surfaces of the substrates. By considering the highly effective, eco-friendly and low-cost nature of the high-power UV-irradiation method, it proved significant potential for industrial mass-production of high-performance adhesive joints of thermoplastic composites.

CRediT authorship contribution statement

Dong Quan: Investigation, Writing - original draft, Funding acquisition. **René Alderliesten:** Funding acquisition, Project administration, Writing - review & editing. **Clemens Dransfeld:** Conceptualization, Resources, Writing - review & editing. **Ioannis Tsakoniatis:** Resources, Investigation. **Sofia Teixeira De Freitas:** Resources, Writing - review & editing. **Gennaro Scarselli:** Resources, Investigation. **Neal Murphy:** Resources, Funding acquisition. **Alojz Ivanković:** Conceptualization, Resources, Funding acquisition. **Rinze Benedictus:** Supervision.

Declaration of competing interest

The authors declare that they have no known competing financial interests or personal relationships that could have appeared to influence the work reported in this paper.

Acknowledgements

Dr. Dong Quan receives funding from the European Union's Horizon 2020 research and innovation programme under the Marie Skłodowska-Curie grant agreement No. 842467. Financial support from the Irish Composites Centre is acknowledged. Special thanks to Dr. Brian Deegan (from Henkel Ireland Operations & Research Ltd., Ireland) and Mr. Lorcán Byrne (from EnBio Ltd., Ireland) for their contribution to the work through valuable technical assistance and discussions.

References

- [1] T. Zhao, G. Palardy, I. Fernandez Villegas, C. Rans, M. Martinez, R. Benedictus, Mechanical behaviour of thermoplastic composites spot-welded and mechanically fastened joints: A preliminary comparison, *Composites B* 112 (2017) 224–234, <http://dx.doi.org/10.1016/j.compositesb.2016.12.028>.
- [2] S.D. Thoppul, J. Finegan, R.F. Gibson, Mechanics of mechanically fastened joints in polymer-matrix composite structure- A review, *Compos. Sci. Technol.* 69 (3) (2009) 301–329, <http://dx.doi.org/10.1016/j.compscitech.2008.09.037>.
- [3] A. Mehboob, S.-H. Chang, Effect of composite bone plates on callus generation and healing of fractured tibia with different screw configurations, *Compos. Sci. Technol.* 167 (2018) 96–105, <http://dx.doi.org/10.1016/j.compscitech.2018.07.039>.
- [4] D. Quan, J.L. Urdaniz, C. Rouge, A. Ivankovic, The enhancement of adhesively-bonded aerospace-grade composite joints using steel fibres, *Compos. Struct.* 198 (2018) 11–18, <http://dx.doi.org/10.1016/j.compstruct.2018.04.071>.
- [5] C. Barile, C. Casavola, G. Pappalettera, P.K. Vimalathithan, Characterization of adhesive bonded CFRP laminates using full-field digital image stereo-correlation and finite element analysis, *Compos. Sci. Technol.* 169 (2019) 16–25, <http://dx.doi.org/10.1016/j.compscitech.2018.10.032>.
- [6] D. Quan, N. Murphy, A. Ivankovic, Fracture behaviour of a rubber nano-modified structural epoxy adhesive: Bond gap effects and fracture damage zone, *Int. J. Adhesion Adhesives* 77 (2017) 138–150, <http://dx.doi.org/10.1016/j.ijadhadh.2017.05.001>.
- [7] R. Tao, X. Li, A. Yudhanto, M. Alfano, G. Lubineau, On controlling interfacial heterogeneity to trigger bridging in secondary bonded composite joints: An efficient strategy to introduce crack-arrest features, *Compos. Sci. Technol.* 188 (2020) 107964, <http://dx.doi.org/10.1016/j.compscitech.2019.107964>.
- [8] C. Ageorges, L. Ye, M. Hou, Advances in fusion bonding techniques for joining thermoplastic matrix composites: A review, *Composites A* 32 (6) (2001) 839–857, [http://dx.doi.org/10.1016/S1359-835X\(00\)00166-4](http://dx.doi.org/10.1016/S1359-835X(00)00166-4).
- [9] E. Tsiangou, S. Teixeira de Freitas, I. Fernandez Villegas, R. Benedictus, Investigation on energy director-less ultrasonic welding of polyetherimide (PEI)-to epoxy-based composites, *Composites B* 173 (2019) 107014, <http://dx.doi.org/10.1016/j.compositesb.2019.107014>.
- [10] X. Li, F. Liu, N. Gong, P. Huang, C. Yang, Enhancing the joining strength of injection-molded polymer-metal hybrids by rapid heating and cooling, *J. Mater. Process. Technol.* 249 (2017) 386–393, <http://dx.doi.org/10.1016/j.jmatprotec.2017.06.034>.
- [11] X. Li, D. Xu, N. Gong, Z. Xu, L. Wang, W. Dong, Improving the strength of injection molded aluminum/polyphenylene sulfide lap joints dependence on surface microstructure and composition, *Mater. Des.* 179 (2019) 107875, <http://dx.doi.org/10.1016/j.matdes.2019.107875>.
- [12] D. Xu, W. Yang, X. Li, Z. Hu, M. Li, L. Wang, Surface nanostructure and wettability inducing high bonding strength of polyphenylene sulfide-aluminum composite structure, *Appl. Surf. Sci.* 515 (2020) 145996, <http://dx.doi.org/10.1016/j.apsusc.2020.145996>.
- [13] A. Pramanik, A. Basak, Y. Dong, P. Sarker, M. Uddin, G. Littlefair, A. Dixit, S. Chattopadhyaya, Joining of carbon fibre reinforced polymer (CFRP) composites and aluminium alloys-a review, *Composites A* 101 (2017) 1–29, <http://dx.doi.org/10.1016/j.compositesa.2017.06.007>.
- [14] A.J. Kinloch, *Adhesion and Adhesives: Science and Technology*, Chapman and Hall, 1987.
- [15] S. Deng, L. Djukic, R. Paton, L. Ye, Thermoplastic/epoxy interactions and their potential applications in joining composite structures - A review, *Composites A* 68 (2015) 121–132, <http://dx.doi.org/10.1016/j.compositesa.2014.09.027>.
- [16] M. Silverstein, O. Breuer, Relationship between surface properties and adhesion for etched ultra-high-molecular-weight polyethylene fibers, *Compos. Sci. Technol.* 48 (1) (1993) 151–157, [http://dx.doi.org/10.1016/0266-3538\(93\)90131-Y](http://dx.doi.org/10.1016/0266-3538(93)90131-Y).
- [17] S. Tiwari, J. Bijwe, S. Panier, Tribological studies on polyetherimide composites based on carbon fabric with optimized oxidation treatment, *Wear* 271 (9) (2011) 2252–2260, <http://dx.doi.org/10.1016/j.wear.2010.11.052>.
- [18] A. Popelka, I. Krupa, I. Novak, M.A.S.A. Al-Maadeed, M. Ouederni, Improvement of aluminum/polyethylene adhesion through corona discharge, *J. Phys. D: Appl. Phys.* 50 (3) (2016) 035204, <http://dx.doi.org/10.1088/1361-6463/50/3/035204>.

- [19] A. Popelka, I. Novák, M.A.S. Al-Maadeed, M. Ouederni, I. Krupa, Effect of corona treatment on adhesion enhancement of LLDPE, *Surf. Coat. Technol.* 335 (2018) 118–125, <http://dx.doi.org/10.1016/j.surfcoat.2017.12.018>.
- [20] V. Fombuena, J. Balart, T. Boronat, L. Sánchez-Nácher, D. García-Sanoguera, Improving mechanical performance of thermoplastic adhesion joints by atmospheric plasma, *Mater. Des.* 47 (2013) 49–56, <http://dx.doi.org/10.1016/j.matdes.2012.11.031>.
- [21] X. Jin, W. Wang, C. Xiao, T. Lin, L. Bian, P. Hauser, Improvement of coating durability, interfacial adhesion and compressive strength of UHMWPE fiber/epoxy composites through plasma pre-treatment and polypyrrole coating, *Compos. Sci. Technol.* 128 (2016) 169–175, <http://dx.doi.org/10.1016/j.compscitech.2016.03.026>.
- [22] M.B. Borooj, A.M. Shoushtari, A. Haji, E.N. Sabet, Optimization of plasma treatment variables for the improvement of carbon fibres/epoxy composite performance by response surface methodology, *Compos. Sci. Technol.* 128 (2016) 215–221, <http://dx.doi.org/10.1016/j.compscitech.2016.03.020>.
- [23] S. Farris, S. Pozzoli, P. Biagioni, L. Duo, S. Mancinelli, L. Piergiovanni, The fundamentals of flame treatment for the surface activation of polyolefin polymers - A review, *Polymer* 51 (16) (2010) 3591–3605, <http://dx.doi.org/10.1016/j.polymer.2010.05.036>.
- [24] D.F. Williams, M.-L. Abel, E. Grant, J. Hrachova, J.F. Watts, Flame treatment of polypropylene: A study by electron and ion spectroscopies, *Int. J. Adhesion Adhesives* 63 (2015) 26–33, <http://dx.doi.org/10.1016/j.ijadhadh.2015.07.009>.
- [25] D.A. Bolon, C.O. Kunz, Ultraviolet depolymerization of photoresist polymers, *Polym. Eng. Sci.* 12 (2) (1972) 109–111, <http://dx.doi.org/10.1002/pen.760120206>.
- [26] J.R. Vig, UV/ozone cleaning of surfaces, *J. Vac. Sci. Technol. A* 3 (3) (1985) 1027–1034, <http://dx.doi.org/10.1116/1.573115>.
- [27] M.J. Walzak, S. Flynn, R. Foerch, J.M. Hill, E. Karbushewski, A. Lin, M. Strobel, UV and ozone treatment of polypropylene and poly(ethylene terephthalate), *J. Adhes. Sci. Technol.* 9 (9) (1995) 1229–1248, <http://dx.doi.org/10.1163/156856195X01012>.
- [28] M.D. Romero-Sanchez, M.M. Pastor-Blas, J.M. Martin-Martinez, M.J. Walzak, UV Treatment of synthetic styrene-butadiene-styrene rubber, *J. Adhes. Sci. Technol.* 17 (1) (2003) 25–45, <http://dx.doi.org/10.1163/15685610360472420>.
- [29] M.D. Landete-Ruiz, J.M. Martin-Martinez, Improvement of adhesion and paint ability of EVA copolymers with different vinyl acetate contents by treatment with UV-ozone, *Int. J. Adhesion Adhesives* 58 (2015) 34–43, <http://dx.doi.org/10.1016/j.ijadhadh.2015.01.003>.
- [30] W. Wang, J.A. Poulis, S. Teixeira de Freitas, D. Zarouchas, Surface pretreatments on CFRP and titanium for manufacturing adhesively bonded bi-material joints, in: *Proceedings of the 18th European Conference on Composite Materials*, Athens, Greece, 2018.
- [31] I. Mathieson, R. Bradley, Improved adhesion to polymers by UV/ozone surface oxidation, *Int. J. Adhesion Adhesives* 16 (1) (1996) 29–31, [http://dx.doi.org/10.1016/0143-7496\(96\)88482-X](http://dx.doi.org/10.1016/0143-7496(96)88482-X).
- [32] H. Shi, J. Sinke, R. Benedictus, Surface modification of PEEK by UV irradiation for direct co-curing with carbon fibre reinforced epoxy prepregs, *Int. J. Adhesion Adhesives* 73 (2017) 51–57, <http://dx.doi.org/10.1016/j.ijadhadh.2016.07.017>.
- [33] BSENISO 10365:1995, *Adhesives-Designation of Main Failure Patterns*, (BS EN ISO 10365:1995) BSI, 1995.
- [34] F. Cheng, Y. Hu, Z. Lv, G. Chen, B. Yuan, X. Hu, Z. Huang, Directing helical CNT into chemically-etched micro-channels on aluminum substrate for strong adhesive bonding with carbon fiber composites, *Composites A* 135 (2020) 105952, <http://dx.doi.org/10.1016/j.compositesa.2020.105952>.
- [35] D. Quan, B. Deegan, L. Binsfeld, X. Li, J. Atkinson, A. Ivankovic, N. Murphy, Effect of interlayering UV-irradiated PEEK fibres on the mechanical, impact and fracture response of aerospace-grade carbon fibre/epoxy composites, *Composites B* 191 (2020) 107923, <http://dx.doi.org/10.1016/j.compositesb.2020.107923>.
- [36] A. Kinloch, *Durability of Structural Adhesives*, Applied Science Publishers Ltd, 1983.
- [37] S. Ebnesajjad, Surface tension and its measurement, in: S. Ebnesajjad (Ed.), *Handbook of Adhesives and Surface Preparation*, in: *Plastics Design Library*, William Andrew Publishing, Oxford, 2011, pp. 21–30, <http://dx.doi.org/10.1016/B978-1-4377-4461-3.10003-3>.
- [38] A.J. Kinloch, C.M. Taig, The adhesive bonding of thermoplastic composites, *J. Adhes.* 21 (3–4) (1987) 291–302, <http://dx.doi.org/10.1080/00218468708074976>.
- [39] G.K.A. Kodokian, A.J. Kinloch, Surface pretreatment and adhesion of thermoplastic fibre-composites, *J. Mater. Sci. Lett.* 7 (6) (1988) 625–627, <http://dx.doi.org/10.1007/BF01730315>.
- [40] A.J. Kinloch, G.K.A. Kodokian, J.F. Watts, The adhesion of thermoplastic fibre composites, *Philos. Trans. R. Soc. Lond. Ser. A Math. Phys. Eng. Sci.* 338 (1649) (1992) 83–112, <http://dx.doi.org/10.1098/rsta.1992.0004>.
- [41] W. Kauzmann, H. Eyring, The viscous flow of large molecules, *J. Am. Chem. Soc.* 62 (11) (1940) 3113–3125, <http://dx.doi.org/10.1021/ja01868a059>.
- [42] J. Xie, A.M. Waas, M. Rassaian, Estimating the process zone length of fracture tests used in characterizing composites, *Int. J. Solids Struct.* 100 (2016) 111–126, <http://dx.doi.org/10.1016/j.ijsolstr.2016.07.018>.
- [43] C. Fan, P.-Y.B. Jar, J.R. Cheng, Cohesive zone with continuum damage properties for simulation of delamination development in fibre composites and failure of adhesive joints, *Eng. Fract. Mech.* 75 (13) (2008) 3866–3880, <http://dx.doi.org/10.1016/j.engfracmech.2008.02.010>.